FeON-FeOFF: the *Helicobacter pylori* Fur regulator commutates iron-responsive transcription by discriminative readout of opposed DNA grooves

Francesca Agriesti, Davide Roncarati, Francesco Musiani, Cristian Del Campo, Mario Iurlaro, Francesca Sparla, Stefano Ciurli, Alberto Danielli* and Vincenzo Scarlato

Department of Pharmacy and Biotechnology (FaBiT), University of Bologna, 40126 Bologna, Italy

ABSTRACT

Most transcriptional regulators bind nucleotide motifs in the major groove, although some are able to recognize molecular determinants conferred by the minor groove of DNA. Here we report a transcriptional commutator switch that exploits the alternative readout of grooves to mediate opposite output regulation for the same input signal. This mechanism accounts for the ability of the *Helicobacter pylori* Fur regulator to repress the expression of both iron-inducible and iron-repressible genes. When iron is scarce, Fur binds to DNA as a dimer, through the readout of thymine pairs in the major groove, repressing iron-inducible transcription (FeON). Conversely, on iron-repressible elements the metal ion acts as corepressor, inducing Fur multimerization with consequent minor groove readout of AT-rich inverted repeats (FeOFF). Our results provide first evidence for a novel regulatory paradigm, in which the discriminative readout of DNA grooves enables to toggle between the repression of genes in a mutually exclusive manner.

INTRODUCTION

Fifty years ago the grounding work of Jacob and Monod set the fundaments for a thorough understanding of gene regulation, postulating the interaction of specialized genetic determinants, *i.e.* operators and regulators, which control gene transcription through the action of signal molecules or cofactors (1). On one hand, these cofactors can act as inducers of transcription, triggering repressor dissociation from the operator element. Conversely, in repressible systems the soluble cofactors induce allosteric conformational changes that prompt a specific DNA binding of the repressor to its regulatory elements. Classic examples are represented by the regulation of the *lac* operon, where the decrease of DNA binding affinity of the Lac repressor is induced by allolactose (2) and by the regulation of the *Escherichia coli trp* operon corepressed by tryptophan and TrpR (3), respectively.

Accordingly, transcription factors regulate gene expression by modulating their DNA binding affinity in response to the cofactor concentration, much akin to inducible or repressible ON-OFF switches. An interesting example is represented by the native and mutagenized forms of the Tet trans-activator (tTA and rtTA), which provide, respectively, the molecular mechanism behind the widely used TetOFF and TetON systems, permitting to switch between the activities of two genes in a mutually exclusive manner (4). Interestingly, some transcription factors combine in one regulator both inducible and corepressible functions in response to the same regulatory cofactor, functioning as molecular commutator switches.

Metal ions are essential for many biological functions and enzymes. At the same time, their overload may induce lethal cytotoxicity. Accordingly, iron homeostasis is tightly regulated in most organisms, playing a key role in host–pathogen interactions (5,6). In the human gastric pathogen *Helicobacter pylori*, an orthologue of the ferric uptake regulator Fur (the quintessential regulator of iron metabolism in many bacteria) is able to repress the transcription of both iron-repressible (FeOFF) and iron-inducible (FeON) promoters (7,8). By this mechanism, like in the TetOFF-TetON system, the same input information translates into two opposite transcriptional outputs. Growing evidence suggests that in the Fur
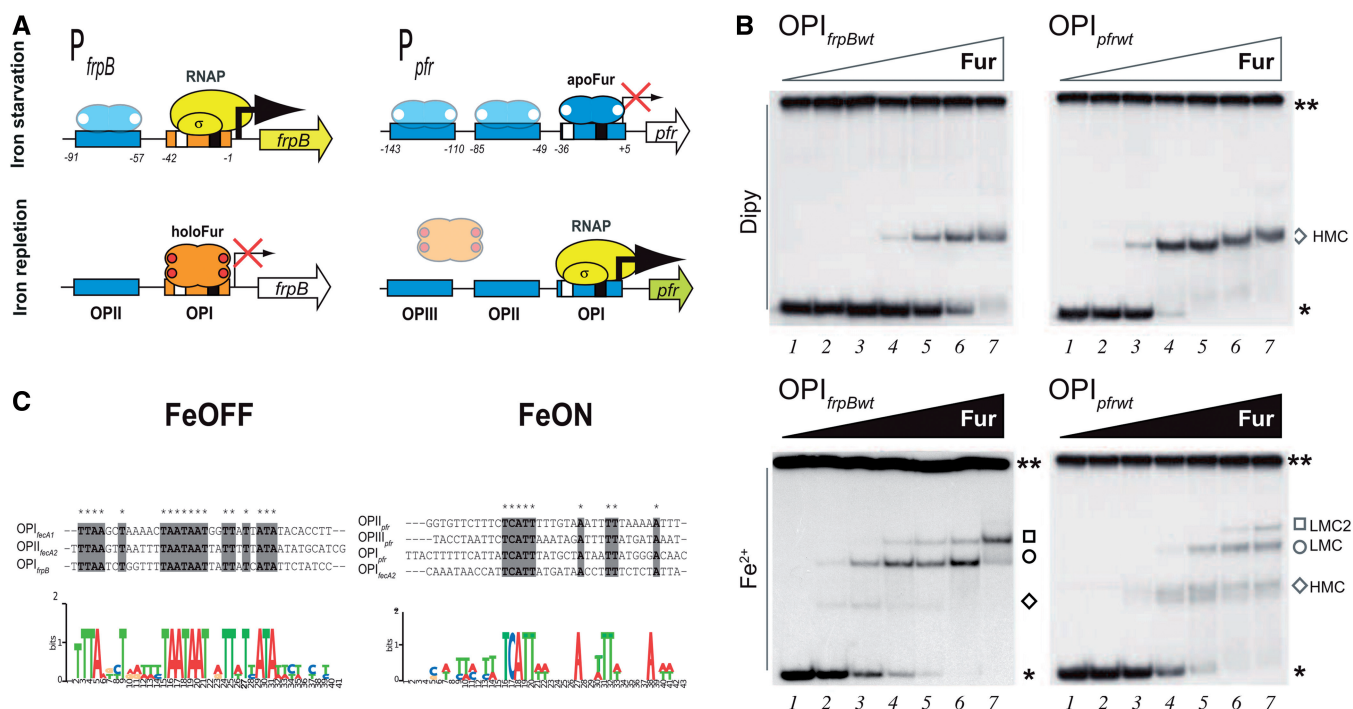

Figure 1. Different Fur binding stoichiometry and operator consensus motifs involved in FeOFF-FeON regulation. (**A**) *Hp*Fur can directly regulate the transcription of both the iron-repressible *frpB1* (FeOFF) and the iron-inducible *pfr* (FeON) genes, according to the metallation state of the protein, through affinity variations for specific operators in their promoters. In both cases, the promoters are derepressed in *fur* mutants. The sites with highest affinity span the −10 and/or −35 core promoter elements, whereas the lower affinity Fur binding sites are located further upstream from the primary Fur box. This fosters the current model of Fur competing with the RNA polymerase for binding to target promoters. (**B**) Gel shifts with OPI$_{frpB}$ and OPI$_{pfr}$ probes represent archetypal examples of Fur-DNA complexes with *holo-* or *apo*-Fur operator elements. Increasing amounts of Fur protein were incubated with end-labelled probes in presence of 150 μM 2,2 dipyridyl (Dipy) and 150 μM soluble Fe^{2+}. Lanes 1–7; 0, 1.2, 2.4, 4.8, 9.6, 18, 39 nM Fur added, respectively. Single asterisks indicate free probe, double asterisks indicate free radiolabeled pBS vector used as non-specific competitor in binding reactions. HMC and LMC denote the high and low mobility complexes formed in a metal-dependent manner, respectively. (**C**) Sequence alignment for *holo*-Fur (FeOFF) and *apo*-Fur (FeON)-specific operators. Asterisks above the sequence alignments indicate conserved bases (grey boxes). Alignments were used to identify a consensus motif, sketched with WebLOGO. Coloured figure available in online version.

family of regulators this type of transcriptional commutation is more widespread than expected (see later in text). Despite the fundamental interest, the mechanisms through which such an alternative regulation can be achieved have not been addressed in detail. Herein, we use the well-studied *H. pylori* Fur as a model to ask how a transcription factor can act as commutator switch.

In particular, when Fe^{2+} is abundant, transcription is repressed by *Hp*Fur in an iron-dependent manner, conforming to the classic Fe^{2+}–Fur (*holo*-Fur) repression paradigm (9), in which the iron ion acts as corepressor (FeOFF; Figure 1A). Accordingly, the iron-repressible Fur targets include genes involved in Fe^{2+} uptake, such as the prototypical *frpB1* gene, which needs to be expressed only under iron-starving conditions (10). On the other hand, when Fe^{2+} is scarce, *Hp*Fur represses transcription of a different set of genes, including the iron-inducible *pfr* gene, which codes for a ferritin involved in iron storage, thus demanding derepression only under iron-replete conditions (11). In this case, the Fe^{2+} cofactor ion acts as an inducer, rather than a corepressor (FeON). This action is mediated by the binding of *apo*-Fur to the OPI$_{pfr}$ operator with a higher affinity when intracellular iron is scarce (10) (Figure 1A). This mode is referred to as *apo*-regulation (or *apo*-repression) (12), which is also involved in the regulation of the superoxide dismutase

sodB gene promoter (13,14). In addition, three operators, recognized with different affinities by *holo*- and/or *apo*-Fur, have been shown to be important for the autorepression mechanism of the *fur* gene itself (15,16).

Importantly, recent studies have indicated that *apo*-regulation in the Fur-family of regulators is not an oddity unique to *H. pylori*. A transcriptional and crystallographic study in *Campylobacter jejuni* suggests that *apo*-regulation may be mediated by a defined orientation and conformation of the DNA binding domains (DBDs) in the *apo*-Fur dimer (17). In *Corynebacterium glutamicum*, the zinc uptake regulator Zur represses the transcription of both zinc-inducible and zinc-repressible genes, acting as a ZnON-ZnOFF commutator switch (18). In analogy, also the iron–sulfur transcription factor IscR of *E. coli* has been reported to exhibit different DNA binding specificities both in its cluster-less (*apo*-IscR) and its cofactored ([2Fe-2S]-IscR) forms (19,20). In all these cases, the use of a single commutator switch supersedes the need for two simple ON-OFF switches. This is particularly relevant to an organism such as *H. pylori*, which codes only for a few transcriptional regulators that appear to be densely interlinked (21). *Hp*Fur acts as global regulator in the transcriptional regulatory network of the bacterium, targeting >200 loci *in vivo* (22), and feeding into the regulatory pathways of many *H. pylori* metabolic processes (8).

The FeON-FeOFF regulation impacts also on the pathogenicity of *H. pylori* because *Hp*Fur, like the Fur orthologs of other bacteria, has an important role in the regulation of the expression of many virulence-associated factors, or contributes to the bacterial fitness, as exemplified by the observed competitive colonization defects of *H. pylori fur* mutants (23).

The molecular details behind transcriptional commutator switches like *Hp*Fur remain largely uncharacterized. The observation that in *H. pylori* the Fur operators of iron-inducible promoters do not share the same motifs of iron-repressible promoters (10,24) fostered the hypothesis that the mechanism may entail two different DNA sequence determinants. Consistently, the Fur orthologs of *Bradyrhizobium japonicum* (*Bj*Fur) and *Borrelia burgdorferi* (*Bb*BosR) can recognize multiple operator typologies (25,26). In this study, we show that the mechanism responsible for the FeON-FeOFF commutation switching in *H. pylori* appears to reside in an allosteric multimerization event induced by Fe^{2+}, which modulates the Fur-dependent readout of *apo*- or *holo*-operator determinants involving different grooves of the DNA helix.

MATERIALS AND METHODS

Full details of the experimental procedures used in this work are presented in Supplementary Data.

Purification of recombinant HpFur

Expression and purification of *H. pylori* Fur was carried out as previously described (27).

Electrophoretic Mobility Shift Assay

Fur-DNA binding reactions were carried out for 15 min, at room temperature, in electrophoretic mobility shift assay (EMSA) buffer [50 mM NaCl; 10 mM Tris (pH 8.0); 10 mM KCl; 0.01% IGEPAL; 10% glycerol; 5 mM DTT] in presence of 50-fold excess of plasmid DNA as non-specific competitor. Approximately 0.6 nM of radiolabelled target DNA and increasing concentrations of Fur, ranging from 0 to 40 nM monomer, were incubated in a final volume of 15 μl. Depending on the effect analysed the buffer was supplemented 150 μM $(NH_4)_2Fe(SO_4)_2 \cdot 6H_2O$ or 150 μM 2,2'-dipyridyl. Binding reactions were resolved on native 6% polyacrylamide gel and electrophoresed in 60 mM Tris, 240 mM boric acid (pH 8.0).

Determination of Fur oligomerization

The multimeric state of pure recombinant Hp*Fur* was estimated by size-exclusion chromatography on a Superdex 200 HR10/30 column connected to an ÄKTA purifier system (GE Healthcare). An EMSA-based method for determining the molecular weights of Fur-DNA complexes was done by performing the Ferguson analysis using a native PAGE molecular weight marker kit.

Hydroxyl radical footprinting

Approximately 0.6 nM of labelled probe was incubated with increasing concentration of Fur in footprinting buffer [50 mM NaCl, 10 mM KCl, 10 mM Tris–HCl (pH 8.0), 0.01% Igepal CA-630, 0.1 mM DTT] at room temperature for 15 min using 300 ng of salmon sperm DNA (Invitrogen) as non-specific competitor in a final volume of 30 μl. The cutting reaction was carried out by the addition of 2 μl each of the following solutions: 125 mM Fe $(NH_4)_2(SO_4)_2$-250 mM EDTA, 1% H_2O_2 and 0.1 M DTT. After 2 min the reaction was quenched by the addition of 25 μl of •OH stop buffer [4% glycerol, 0.6 M sodium acetate (pH 5.2), 100 μg ml^{-1} sonicated salmon sperm DNA], phenol-chloroform extracted and ethanol precipitated. Samples were resuspended in 6 μl formamide loading buffer, denatured at 92°C for 2 min, separated on 8 M urea-8.5% acrylamide sequencing gels and autoradiographed.

Distamycin A interference assays

For interference assays *in vitro*, DNA probes (0.6 nM) were preincubated for 15 min at 22°C with 1.2, 2.4, 4.8 nM distamycin A in 10 μl EMSA buffer. Then, Fur was added to the reaction for an additional 15 min incubation, before complex separations by EMSA. For interference *in vivo*, mid-log phase *H. pylori* cultures were preincubated for 20 min with 20 μM distamycin A and subsequently treated for 15 min with either 1 mM $(NH_4)_2Fe(SO_4)_2 \cdot 6H_2O$ [Fe^{2+}] or 150 μM 2,2'-dipyridyl [Dipy], before RNA extraction and qRT-PCR analysis.

Construction of lacZ transcriptional fusions and primer extension analysis

Transcriptional fusions with *lacZ* (Supplementary Table S1) were inserted into the *vacA* locus on the chromosome of both wild-type and *Δfur H. pylori* strains by homologous recombination. Correct integrations were confirmed by PCR using primers FfrpB_wt and A3Z2 (Supplementary Table S2). Total RNA was extracted by a hot-phenol procedure (28); primers BZ9 and BZ10 were used for primers extension experiments, using previously described procedures (27).

Native Fur modelling and unbound DNA structure generation

The crystal structure of the dimeric form of a mutant *H. pylori holo*-Fur bound to Zn^{2+} ions (29) (PDB: 2XIG) was used as template structure to calculate the model structure of the dimer of native *Hp*Fur using MODELLER 9v8. The best model was selected on the basis of the lowest value of the DOPE score and subjected to a refining step of loop optimization. The stereochemical quality of the structures was established using PROCHECK, and the distribution of residual energy was evaluated in ProSA (Supplementary Table S3) (30). The *apo*-Fur model structure was obtained by depletion of Zn^{2+} ions from the model structure of *holo*-Fur. The five low-frequency normal conformational modes of *apo*- and *holo*-Fur of the *H. pylori* model structure were calculated

using the elNémo web-server (31). Derivative protein conformations were used to build a library of structures to be used in subsequent docking calculations. The obtained structures are reported in Supplementary Figure S5. Models for unbound *holo-* and *apo-*operators were generated using the DNA analysis and rebuilding software 3DNA implemented in the 3D-DART server (32). The models were generated in canonical B-DNA conformation.

Protein–DNA docking

The *Hp*Fur model structure library was docked to *holo-* and *apo-*operators using the data-driven docking programme HADDOCK 2.1, adopting a two-stage protein–DNA docking approach (33). In the first docking round, a rigid body energy minimization was carried out, 1000 structures were calculated and the 200 best solutions based on the intermolecular energy were used for the semi-flexible, simulated annealing followed by an explicit water refinement. The solutions were clustered using a cut-off of 7.5 Å RMSD based on the pair wise backbone RMSD matrix. Additional restraints were introduced for the DNA to maintain base planarity and Watson–Crick bonds. A second docking round was carried out including the ensemble of custom DNA models generated, whereby the conformational freedom of the DNA molecule was restricted at the semi-flexible refinement stage to prevent helical deformation. If pertinent with experimental evidences, additional restraints were applied to take into account the symmetry of the complex and to bring the protein in contact to interacting DNA bases or nucleotides (Supplementary Table S4).

RESULTS

The iron cofactor determines different binding stoichiometry of Fur to DNA

To study the role of the iron cofactor on the DNA binding mechanism of *Hp*Fur, we carried out EMSA on short DNA probes, 64 and 62 bp in length, containing the OPI_{frpB} and OPI_{pfr} operator sequences, mediating iron-repressible (FeOFF) and iron-inducible (FeON) Fur regulation, respectively. Both operator probes were incubated with increasing concentrations of purified Fur protein in the presence of either a free Fe^{2+} (150 μM) or a specific Fe^{2+} chelator (150 μM 2-2' dipyridyl), and protein–DNA complexes were separated on non-denaturing polyacrylamide gel electrophoreses (Figure 1B). The obtained results are consistent with the opposite effect of Fe^{2+} ions on the affinity of Fur towards operators isolated from the multioperator context, with Fur exhibiting a 10-fold decrease for OPI_{frpB} (FeOFF) and a 4-fold increase in affinity for OPI_{pfr} (FeON) in response to iron chelation (Figure 1B and Table 1).

In addition, two low-mobility complexes, LMC and LMC2 were preferentially formed in the presence of Fe^{2+}, whereas a single high-mobility complex (HMC) was formed by Fur in response to Fe^{2+}-chelation (Figure 1B). Thus, the presence/absence of Fe^{2+} determines the formation of different Fur-DNA complexes. Size exclusion chromatography indicated that the Fur protein used in our binding studies is a dimer in solution and that it is able to tetramerize, and further multimerize, in the presence of divalent metal ions (Fe^{2+} and Mn^{2+}), even in the absence of DNA (Supplementary Figure S1). To determine the stoichiometry of Fur binding to DNA for the various complexes observed in EMSA, the Ferguson method was used (Supplementary Figure S1). For both OPI_{pfr} and OPI_{frpB} operators, the molecular mass of HMC was estimated as 85 kDa, which is consistent with the expected molecular mass of 76 kDa calculated for a dimer of Fur (~35 kDa) bound to the 64-bp DNA probe. In contrast, the LMC complex showed an apparent molecular mass of 118 kDa, in agreement with the expected molecular mass of 110 kDa calculated for two dimers of Fur bound to the DNA operators. Finally, the LMC2 resulted in a complex of 228 kDa, a molecular mass that is similar to the predicted value of 220 kDa for two Fur tetramers, each bound to an operator probe.

These results suggest that *apo*-Fur binds DNA preferentially as a dimer, whereas *holo*-Fur binds DNA as a tetramer, and that two *holo*-Fur tetramers can interact with each other without losing contacts to the bound operators. The ability of Fur to form these higher order structures reminds that observed in the case of *Bj*Fur (25), and is in agreement with previous observations of Fur multimerization in *H. pylori*, both *in vivo* and *in vitro* (12,15,34). Therefore, regardless of the operator typology specifically recognized by the protein, the binding stoichiometry of Fur to DNA is a function of the metallation state of the protein, although the specific operator sequences provide the determinants underlying distinct binding affinities of Fur in response to iron.

Table 1. Fur affinity constants (nM) to iron-inducible and iron-repressible elements

Element	Sequence	K_A *holo*-Fur	K_A *apo*-Fur
OPI_{pfr}	TTACTTTTTCATTA<u>TCATT</u>TATGCTATAA<u>TT</u>ATGGGACAAC	5.6 ± 1.6	1.3 ± 0.3
$OPI_{pfr\ C17A}$	TTACTTTTTCATTAT**A**ATTTATGCTATAA<u>TT</u>ATGGGACAAC	n.d. (>20.0)	n.d. (>20.0)
OPI_{frpB}	TTTTAATCTGGTTT<u>TAATAATAATTATCA</u>TACTATTCTATCCC	2.4 ± 0.1	n.d. (>20.0)
$OPI_{frpB\ ind}^{+}$	TTTTAATCT**CA**TTT<u>TAATAATAATTATCA</u>TACTATTCTATCCC	5.3 ± 2.6	14.2 ± 6.4
$OPI_{frpB\ rep}^{-}$	TTTTAATCTGGTTT<u>TA**CTAC**TAATTATCA</u>TACTATTCTATCCC	10.3 ± 1.7	n.d. (>20.0)
$OPI_{frpB\ rep}^{-}{}_{ind}^{+}$	TTTTAATCT**CA**TTT<u>TA**CTAC**TAATTATCA</u>TACTATTCTATCCC	11.4 ± 1.3	6.3 ± 0.4

Mutagenized nucleotides are shaded in black. The consensus motifs for the $TCATT_{n10}TT$ element and the $TAATAAT_nATTATTA$ inverted repeat are underscored. Affinity constants (K_A = 50% bound probe) were obtained by best-fitting to the Hill equation the EMSA isotherms obtained, respectively, in the presence of 150 μM soluble Fe^{2+} (*holo*-Fur) or 150 μM 2,2 dipyridyl chelator (*apo*-Fur). Errors represent the standard deviation for K_A deriving from ≥3 independent experiments; n.d. affinity constants > 20 nM are not determined.

TCATT$_{n10}$TT: a consensus motif for the recognition of operators bound with higher affinity by *apo*-Fur

To identify sequence-specific determinants within the two operator typologies, we first expanded the set of workable operators, by characterizing three additional operators found in the P$_{fecA1}$ and P$_{fecA2}$ promoters, known to be regulated by Fe^{2+} in a Fur-dependent manner (27); see also Supplementary Figure S2). The sequences of the three operators bound with higher affinity by *holo*-Fur (OPI$_{frpB}$, OPI$_{fecA1}$ and OPII$_{fecA2}$) and those of the four operators (OPI$_{pfr}$, OPII$_{pfr}$, OPIII$_{pfr}$ and OPI$_{fecA2}$) recognized with higher affinity by *apo*-Fur were aligned and a consensus sequence was defined (Figure 1C). For the operators recognized with higher affinity by *holo*-Fur, this analysis revealed an AT-rich nucleotide stretch organized in a TAATAAT$_n$ATTATTA inverted repeat, as also recently observed in an independent study (24). By contrast, sequence analysis of the operators recognized by *apo*-Fur revealed the peculiar consensus motif TCATT, separated by a gap of 10 nucleotides from a thymine dimer (TCATT$_{n10}$TT, Figure 1C).

 A motif scan search with RSAT (35), identified 393 copies of this motif in the 26 695 *H. pylori* genome. Analysis of these hits with the results of genome-wide Fur ChIP data sets (22) indicated that this motif is present in 94 out of 154 targets of the *apo*-Fur targets predicted by ChIP, including the *apo*-regulated *sodB* promoter (14). Thus, the seven bases of the TCATT-n10-TT motif appear to confer a high-affinity *apo*-Fur binding interaction, although it cannot be excluded that other bases may be involved in the binding. To validate the TCATT$_{n10}$TT motif as the *apo*-Fur consensus in *H. pylori*, we evaluated the binding affinity of *apo*- and *holo*-Fur to mutagenized variants of this element. The obtained results indicate that the unique cytosine in the motif (providing a discriminating element over the AT-rich background of *holo*-Fur operators), together with the precise phasing of the thymine pairs, separated by one helical turn of the DNA, are discriminative elements for high-affinity binding of *apo*-Fur (Table 1; Supplementary Figure S3).

Swapping the iron-dependent Fur binding affinities of a *holo*-operator into an *apo*-operator

The *holo*-Fur-box of *H. pylori* appears as a TAATAAT$_n$ATTATTA inverted repeat. *De novo* introduction of this element in an independent promoter region confers Fur-dependent iron-repressible (FeOFF) regulation (24). To characterize this element, we mutagenized two AAT triplets of one hemi-operator site into two ACT triplets, generating OPI$_{frpB\ rep}^-$. In EMSA, the binding affinity of Fur to this operator mutant exhibited a 4-fold decrease compared with the OPI$_{frpB}$ wild-type probe, a phenomenon that is more evident in Fe^{2+}-replete conditions (Figure 2, compare panel A with panel B, Table 1). This would suggest a loss of function, indicating that the inverted repeat of AAT triplets is an important determinant for the recognition of the *holo*-operator, whereas the TCATT$_{n10}$TT motif identifies the *apo*-operator. These results imply the distinction between the *holo*- and *apo*-elements as two

distinct operator typologies, which may rely on different molecular mechanisms for their correct readout by *apo*- and/or *holo*-Fur, respectively. Intriguingly, the two types of sequences may overlap within the same operator. We identified a consensus for both motifs on the OPI$_{fur}$ operator of the *fur* gene promoter, which is bound with similar affinity by either *holo*-Fur or *apo*-Fur (16). To verify this hypothesis, we reconstituted a TCATT$_{n10}$TT motif within OPI$_{frpB}$ by substitution of only two bases that map outside the TAATAAT$_n$ATTATTA inverted repeat, leaving the *holo*-Fur element intact, generating OPI$_{frpB\ ind}^+$. A marked increase of binding affinity of Fur to this mutagenized element was observed under Fe^{2+} depleting conditions, while only a minor decrease in binding affinity of Fur under Fe^{2+}-replete conditions was detected, suggesting a gain of function of *apo*-Fur for the OPI$_{frpB\ ind}^+$ mutant operator (Table, 1; Figure 2C). Finally, when both mutations were combined in OPI$_{frpB\ rep}^-\ _{ind}^+$ a clear swap in the metal-responsive binding affinity of Fur was observed (Table 1; Figure 2D, compare also isotherms in Supplementary Figure S4).

 These data indicate that the TAATAAT$_n$ATTATTA inverted repeat and the TCATT$_{n10}$TT element may dictate the Fe^{2+}-repressible and Fe^{2+}-inducible Fur-dependent transcriptional regulation *in vivo*, respectively. To verify this hypothesis, we constructed transcriptional fusions of the OPI$_{frpB}$ operator, containing a functional core promoter element, with a downstream promoterless *lacZ* sequence, assayed for transcriptional activity by primer extension analysis (Figure 3). In a parental background, transcription of the OPI$_{frpB}$-*lacZ* fusion is almost completely repressed by Fe^{2+} repletion, whereas Fe^{2+} chelation leads to a marked transcriptional derepression. Conversely, in a Δfur background transcription of OPI$_{frpB}$-*lacZ* is constitutively derepressed. This provides evidence that the OPI$_{frpB}$ *holo*-operator, overlapping a functional −10 promoter region, retains the molecular determinant responsible for Fe^{2+}-repressible Fur regulation in *cis* (Figure 3).

 Subsequently, we investigated the effect of the aforementioned mutations on the iron-dependent regulation of the OPI$_{frpB}$-*lacZ* transcriptional fusions. We could not investigate the iron-responsiveness of OPI$_{frpB\ rep}^-$ because the mutation zeroed transcription from the promoter fusion. By contrast, transcription from the OPI$_{frpB\ ind}^+$ element, in which the reconstituted *apo*-Fur TCATT$_{n10}$TT motif leaves the wild-type *holo*-Fur element intact, significantly mitigated the derepressive effect of Fe^{2+} chelation, without interfering with the Fe^{2+}-repressibility (Figure 3). This gain of function is conferred by *apo*-Fur repression as demonstrated by Fe^{2+}-independent transcriptional derepression of the OPI$_{frpB\ ind}^+$-*lacZ* fusion in a Δfur background. Thus, the insertion of a TCATT$_{n10}$TT motif to OPI$_{frpB\ ind}^+$ attenuates the derepressive effect of iron chelation, reflecting the affinity constants observed *in vitro* (Table 1).

Fur adopts distinctive binding architectures on *holo*- and *apo*-operators

To further characterize the *holo*- and *apo*-Fur-DNA interactions, we performed Fur hydroxyl radical (•OH)
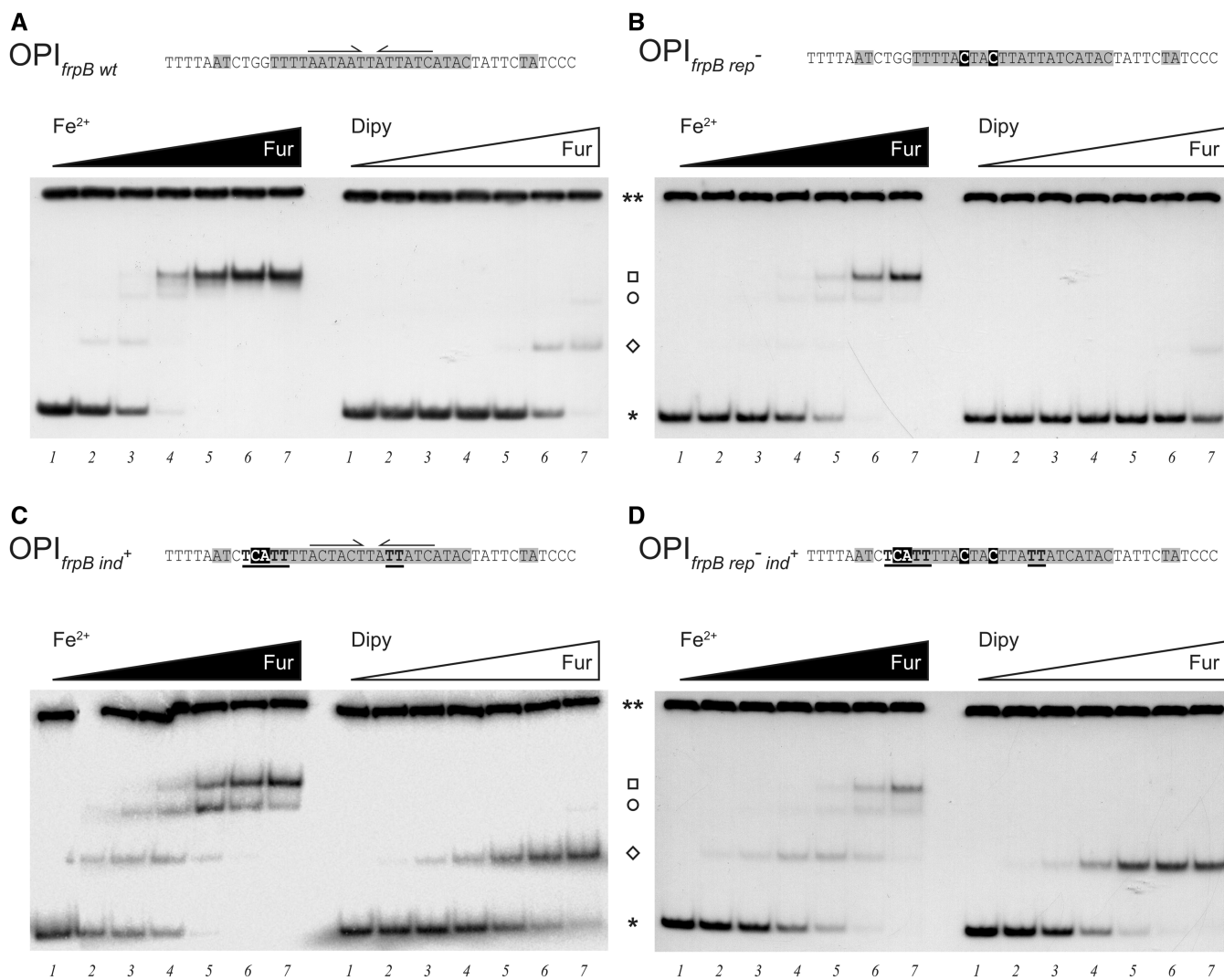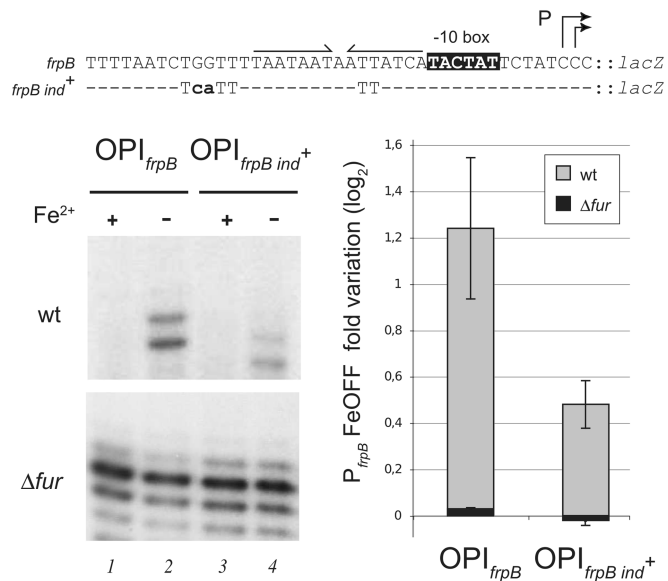
Figure 2. Nucleotide sequences and representative EMSA experiments for wild-type OPI$_{frpB}$ (**A**) or mutated loss of function OPI$_{frpB\ rep}^-$ (**B**), gain of function OPI$_{frpB\ ind}^+$ (**C**) and swapped OPI$_{frpB\ rep^-\ ind}^+$ (**D**) probes. Nucleotides protected from •OH cleavage (data from Figure 4) on the wild-type OPI$_{frpB}$ operator are shaded in grey. Convergent arrows above the sequence indicate the *holo*-operator inverted repeat. Mutated nucleotides are shaded in black. Nucleotides forming a TCATT$_{n10}$TT consensus motif within the OPI$_{frpB}$ *holo*-operator element are underscored in bold letters.

footprinting experiments with P$_{frpB}$ and P$_{pfr}$ promoter probes, in the presence of 150 µM MnCl$_2$ or 150 µM 2,2'-dipyridyl. Mn^{2+} was used as a cofactor instead of Fe^{2+}, as it is more stable, does not interfere with the •OH cleaving reaction and has been shown to function like Fe^{2+} under *in vitro* binding conditions (36).

The obtained results highlight important differences in the interaction of Fur with its operator regions (Figure 4). On *holo*-operators (*e.g.* OPI$_{frpB}$), the binding of Fur results in an extended footprint of 21-bp, mapping within the AT-rich region encompassing the TAATAAT$_n$ATTATTA inverted repeat (Figure 4A and C). Furthermore, at higher concentrations of Fur, two short additional stretches of protection, flanking symmetrically the core of the 21-bp protected region appeared (Figure 4A, lanes 6–7). Similar results have been obtained from the non-coding strand (results plotted in Figure 4C), indicating protein wrapping around the DNA helix, as sketched in Figure 2E. Similar results have been obtained also on

other operators (OPI$_{fecA1}$ and OPII$_{fecA2}$) recognized with higher affinity by *holo*-Fur (Supplementary Figure S2).

In striking contrast, the binding of Fur to *apo*-operators encompassing a TCATT$_{n10}$TT motif (OPI$_{pfr}$, but also OPII$_{pfr}$, OPIII$_{pfr}$ on P$_{pfr}$ and OPII$_{frpB}$ on P$_{frpB}$), resulted in a periodic pattern of four short protected regions of 2/4 nucleotides in length (Figure 4B–D). The two main central regions are separated by 10 ± 1 nucleotides, whereas two flanking stretches, separated by 4–8 nucleotides from the central core, appear at higher protein concentrations. The protected areas on the non-coding strands are offset from those of the coding strands by 1 nucleotide (results plotted in Figure 4D), suggesting that Fur binds only to one face of the DNA helix on these operators (Figure 4F). Remarkably, the bases that are directly protected from •OH cleaving at minimal *apo*-Fur concentration are represented by two thymine dimers separated by a gap of 10 bp (Figure 4B) that correspond to the thymine dimers of the TCATT$_{n10}$TT consensus motif.

P

frpB TTTTAATCTGGTTTT**TAATAATAATTATCA**TA**TACTAT**TCTATCCC::*lacZ*

frpB ind⁺ --------T**ca**TT----------TT------------------::*lacZ*

-10 box

OPI$_{frpB}$ OPI$_{frpB\ ind}$⁺

Fe²⁺   +   −   +   −

wt

Δfur

1   2   3   4

P_{frpB} FeOFF fold variation (log$_2$)

□ wt
■ Δfur

OPI$_{frpB}$ OPI$_{frpB\ ind}$⁺

Figure 3. Reconstitution of a TCATT$_{n10}$TT motif within a *holo*-operator confers *apo*-regulation *in vivo*. Representative *lacZ* primer extensions on total RNA extracted at mid-log growth phase from G27 wild-type (wt) or *fur* knock out (Δ*fur*) strains encompassing the *vacA*::P$_{OPIfrpB}$-*lacZ* transcriptional fusions, with wild-type OPI$_{frpB}$ or the gain-of-function OPI$_{frpB\ ind}$⁺ operator in response to iron repletion [1mM (NH$_4$)$_2$Fe(SO$_4$)$_2$; Fe+] or iron chelation (150 μM 2,2'-dipyridyl; Fe-). Arrows above the OPI$_{frpB}$ nucleotide sequence indicate the inverted repeat of the *holo*-Fur binding consensus motif. Bent arrows mark the transcriptional start site; the mapped −10 box of the promoter is shaded in black. The two mutagenized bases in OPI$_{frpBind}$⁺ are indicated in bold lowercase letters. The FeOFF/FeON transcript ratio is reported in the graph; grey bars: G27 wt genetic background; black bars: Δ*fur* genetic background; vertical bars indicate the standard deviation of three independent replicates.

Chelation of Fe²⁺ by the addition of 2,2'-dipyridyl always results in a pattern of •OH protection induced by Fur that is indistinguishable from that observed after metal ion addition, suggesting that it is the operator to impose the distinctive binding architecture to the regulator (Figure 4A and B), and not its metallation state. In other words, the regulatory metal ion, in accordance with EMSA results (Figure 2A), oppositely influences the affinity of Fur for distinct operator typologies (compare left and right panels in Figure 4A and B), but appears to have little effect on the mode of Fur binding to the latter. The same results were obtained for •OH footprinting experiments performed on operator sequences isolated from the multioperator context of the promoter. This suggests that the different binding architectures of Fur represent a general rule for discriminating *holo*- and *apo*-Fur operators, as verified also by •OH footprinting analysis on to the P$_{fecA1}$ and P$_{fecA2}$ promoters (see Supplementary Figure S2).

According to the aforementioned findings, the operator mutant OPI$_{frpB\ rep^-\ ind}$⁺, which swaps the Fe²⁺-dependent binding affinities of Fur to DNA (Table 1), should also impose a switch on the binding architecture of the regulator. In •OH footprinting experiments with this functionally swapped operator, the Fur binding architecture changed from the typical extended protection pattern,

distinctive of a *holo*-operator, to a periodic pattern of four protected regions separated by ∼10 •OH sensitive base pairs. This pattern is similar to the well-characterized *apo*-operator protection pattern of OPI$_{pfr}$ (Figure 5A). Consistently, Fur protects mainly the thymine dimers separated by 10 nt of the TCATT$_{n10}$TT element reconstituted in OPI$_{frpB\ rep^-\ ind}$⁺, with a periodicity similar to that shown for the *apo*-operator OPI$_{pfr}$ (see grey boxes in Figure 5B).

All together, these results suggest that the nucleotide sequence of each operator dictates the binding architecture of Fur to DNA in *cis*, conferring a molecular determinant for preferential binding by either the *apo* or *holo*-Fur.

Distamycin A interferes with Fur binding to *holo*-operators

Hydroxyl radicals promote DNA strand scission primarily through minor groove abstraction of protons of the de-oxyribose sugar ring (37). Thus, the distinct patterns of protection displayed by Fur on *apo*- and *holo*-operators could testify a different interaction of the regulator with the minor groove of these elements. In this respect, we were intrigued to trace four (2+2) recurring AAT triplets in the *holo*-operator inverted repeat consensus motif: AT-rich sequences, not containing the flexible TpA step, provide a discriminating feature for minor groove shape readout, involving positively charged Arg or Lys residues of DNA binding factors able to interact with the enhanced negative potential of the narrowed minor groove (38).

To investigate this hypothesis, we implemented (DNA binding) interference experiments with distamycin A, a small drug that binds the minor groove of AT-rich DNA. As little as 1.2 nM distamycin proved sufficient to affect Fur binding to the *holo*-operator OPI$_{frpB}$ in EMSA (Figure 6A). At higher drug concentration, a complete inhibition of the Fur-OPI$_{frpB}$ complex formation was observed. Conversely, binding to the OPI$_{pfr}$ *apo*-operator was basically unaffected, with only a slight loss of affinity at the highest distamycin concentration. These results suggest that distamycin A out-competes Fur binding to OPI$_{frpB}$ but not to OPI$_{pfr}$. This is a strong indication that the readout of critical determinants conferred by the minor groove (in addition to other possible major groove contacts) underlies the recognition of *holo*-operators, whereas the recognition of *apo*-operators occurs through the major groove of the DNA, probably as a result of a direct readout of the specific TCATT$_{n10}$TT sequence motif. Accordingly, the binding of Fur to the mutated OPI$_{frpB\ ind}$⁺ *holo*-operator, encompassing a reconstituted TCATT$_{n10}$TT motif conferring iron-inducible repression, proved less sensitive to distamycin and was only partially inhibited at the maximum drug concentration (Figure 6A).

Minor groove readout of *holo*-operator elements

It has been reported that in some cases minor groove binding of distamycin derivatives can allosterically displace regulators bound in the major groove of DNA
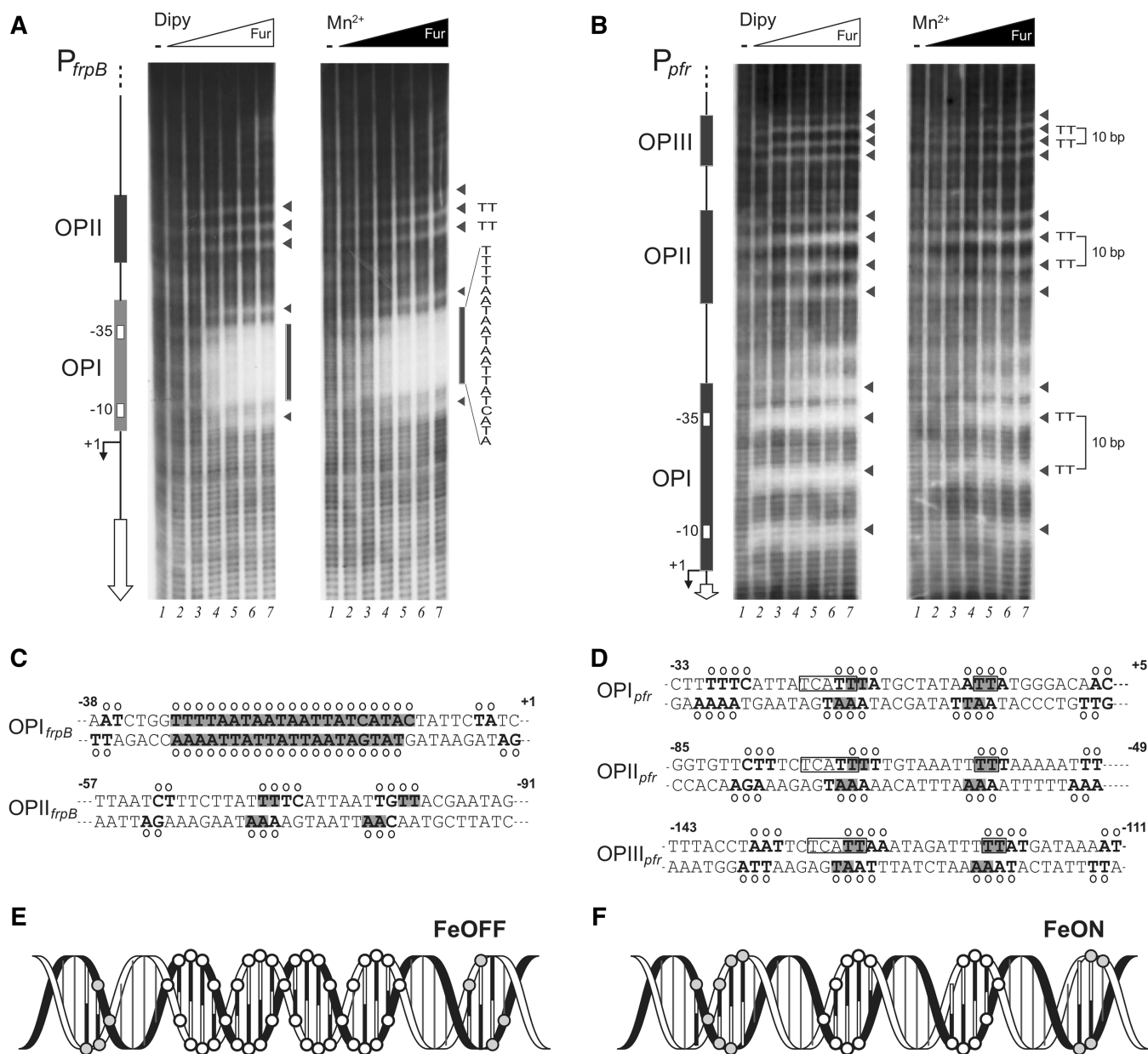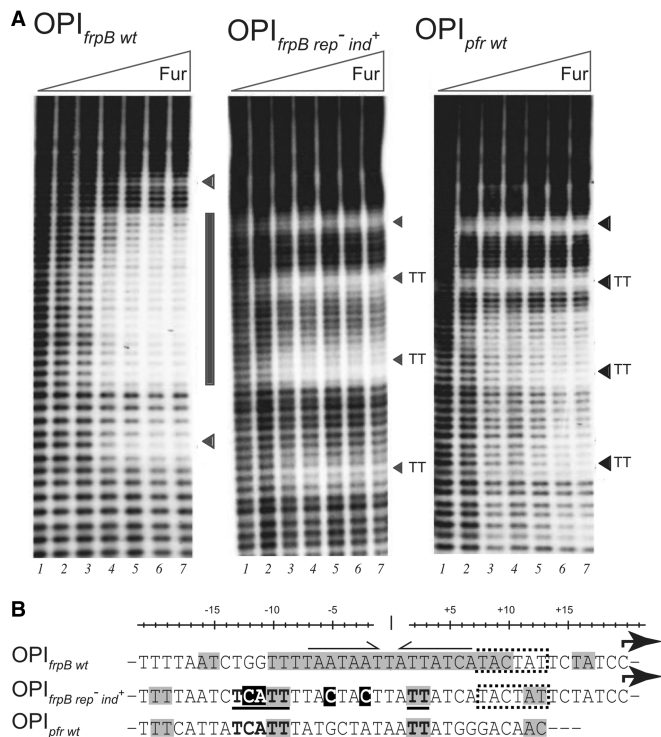
Figure 4. Distinctive binding architecture of Fur to *holo*- and *apo*-operator elements. (**A** and **B**) Specific DNA probes for P_{frpB} (A) and P_{pfr} (B) fragments, end labelled on the coding strand, were incubated with increasing amounts of recombinant Fur protein in presence of 150 μM 2,2'dipyridyl (Dipy, left panel) or in presence of 150 μM $MnCl_2$ (Mn^{2+}, right panel). Lanes 1–7; 0, 29, 61, 122, 244, 490, 980 nM Fur (monomer) added, respectively. Fur binding sites, protected by DNase I, with highest affinity for either *holo*- (light grey boxes) or *apo*-Fur (dark boxes). The open boxes on the right indicate the extended region of •OH protection, whereas the arrowheads indicate short protected areas from •OH cleavage. Bent arrows mark transcriptional start sites, the position of the −10 and −35 hexamers are marked by open rectangles; open reading frames are indicated by vertical open arrows to the left of each gel. (**C** and **D**) Summary of protection data on operators from P_{frpB} (C) and P_{pfr} (D). For each operator, the numbers are referred to the respective transcriptional start site (+1). Open circles indicate bases protected by Fur on the coding or the non-coding strand. Strongly protected bases are shaded in grey. (**E** and **F**) Representative helical projections of the •OH protected residues (open circles) on the OPI_{frpB} (E) and OPI_{pfr} (F) DNA backbone. Shaded and black bars in the DNA helix represent adenine and thymine bases, respectively.

(39). Thus, to prove the involvement of minor grove readout in the discriminative recognition of *holo*-operators, we performed Inosine-Cytosine (I-C) box EMSA experiments. I-C base pairing significantly modifies the charge signature in the major groove, but leaves the electrostatic potential and the shape of the minor groove unaltered (40). We substituted with inosines the two central adenosines of the AAT triplet repeat of the wild-type OPI_{frpB} operator (and complementary cytidine substitutions of thymine), generating $OPI_{frpBI = C}$, (Figure 6B). Because mutations in these positions resulted in a strong decrease in *Hp*Fur binding affinity in EMSA assays with $OPI_{frpB\ rep}^{-}$ (Table 1 and Figure 2B), we expected the affinity of Fur for the inosine-

Figure 5. A swap in the iron-dependent binding affinity changes the binding architecture of Fur to the operator element. (**A**) The •OH footprinting assays on OPI_{frpB}, $OPI_{frpB\ rep^-ind^+}$ and OPI_{pfr} probes. Symbols are described in the legend of Figure 4. (**B**) Sequence alignments of the OPI_{frpB}, $OPI_{frpB\ rep^-ind^+}$ and OPI_{pfr} operators. The four point mutations reconstituting a $TCATT_{n10}TT$ element in a *holo*-Fur loss-of-function operator are shaded in black. The nucleotides protected from •OH cleavage in panel A are shaded in grey. Arrows above the OP_{frpB} nucleotide sequence indicate the inverted repeat of the *holo*-Fur binding consensus motif. Horizontal bars mark the $TCATT_{n10}TT$ elements.

substituted $OPI_{frpB\ I=C}$ probe to decrease, only if the readout of these critical positions occurred in the major groove. Results shown in Figure 6C failed to detect loss of Fur binding affinity on $OPI_{frpB\ I=C}$, consistently with a readout of the minor groove for *holo*-operators. In addition, EMSA experiments performed with I-C box substitutions of the thymine dimers of the $TCATT_{n10}TT$ element of OPI_{pfr} verified a dramatic loss of affinity of Fur (Supplementary Figure S5), suggesting a specific readout in the major groove of the *apo*-operator.

Distamycin A impairs Fe^{2+}-repressible Fur regulation

To assess the involvement of minor groove readout in the regulation of Fur targets, we performed interference assays *in vivo*, verifying the effect of distamycin A on the Fe^{2+}-repressibile (FeOFF) or Fe^{2+}-inducibile (FeON) transcriptional response mediated by Fur, respectively, after Fe^{2+} repletion or chelation (Figure 6D). In response to Fe^{2+} chelation, Fur significantly represses transcription of the iron-inducible *pfr* gene. Similarly, *apo*-Fur repression is essentially maintained in cultures treated with distamycin. On the contrary, distamycin strongly impairs the Fe^{2+}-repressible Fur regulation, as evidenced by the transcriptional derepression of the *frpB*

gene, even under Fe^{2+}-replete conditions. These results suggest that FeOFF, but not FeON, regulation is subordinated to the accessibility of the minor groove by *Hp*Fur readout *in vivo*, providing evidence for a mechanism involving the discriminative recognition of genetic determinants carried on opposed DNA grooves to control the transcription of alternative sets of genes.

Structural modelling of the Fur-DNA interaction

In the absence of cocrystals, we took advantage of a recently solved structure of a *H. pylori* C78S, C150S *holo*-Fur double mutant (29) (PDB code: 2XIG, Supplementary Figure S6A), to model Fur-DNA interactions and gain insight into the mechanism responsible for the distinctive recognition of *apo*- and *holo*-operators. First, we pursued the structural modelling of native Fur from *H. pylori* both in the *holo*- and in the *apo*-form, and applied state-of-the-art coarse-grained computational techniques to compile a library of possible *apo*- and *holo*-Fur conformations (Supplementary Figure S6B and C, see also 'Extended Materials and Methods' in Supplementary Data). Next, the experimental evidences and molecular constraints verified in this study were used to guide the protein–DNA docking simulations through the data-driven HADDOCK programme (41,42).

In the case of protein complexes with the *apo*-operator OPI_{pfr}, the best docking was obtained for an *apo*-Fur/OPI_{pfr} model, which features the axis connecting the two DBDs of the Fur dimer nearly parallel to the DNA major axes (Figure 7A, Supplementary Table S4). In the model, the Fur DBD inserts the loop between helices α1 and α2, as well as the first five residues of helix α4, in the major groove of the *apo*-operator in correspondence with the two regions identified by •OH footprinting assay. The *apo*-operator region comprised between the active bases is predicted to not interact with the protein and assumes a convex conformation with respect to the Fur position, broadening the major grooves exposed to the protein in correspondence of the thymine dimers. The verified protection of the same bases in •OH footprinting assays (Figure 4) argues in favour of this model, as broadening of the major groove is compatible with a distortion (narrowing) of the minor groove.

In the case of complexes with OPI_{frpB}, the best docking was obtained for a tetrameric *holo*-Fur/OPI_{frpB} model, in which two Fur dimers may approach the operator from opposed faces of the DNA, interacting with the axis connecting their DBDs positioned perpendicular to the DNA major axis and covering to a large extent the region of the operator protected in •OH footprinting assays (Figure 7B). Interestingly, several charged residues of the α4 DNA recognition helix of both *holo*-Fur dimers point towards the minor groove of the *holo*-operator (Supplementary Figure S7A), even though the constraints of the docking algorithm were not explicitly set to reward these interactions with the minor groove. In addition, the spacing and electrostatic properties of the residues found on the surface of the DBD of each dimer appear to simmetrically match with each other (Supplementary Figure S7B and C; Supplementary Table S4), in agreement
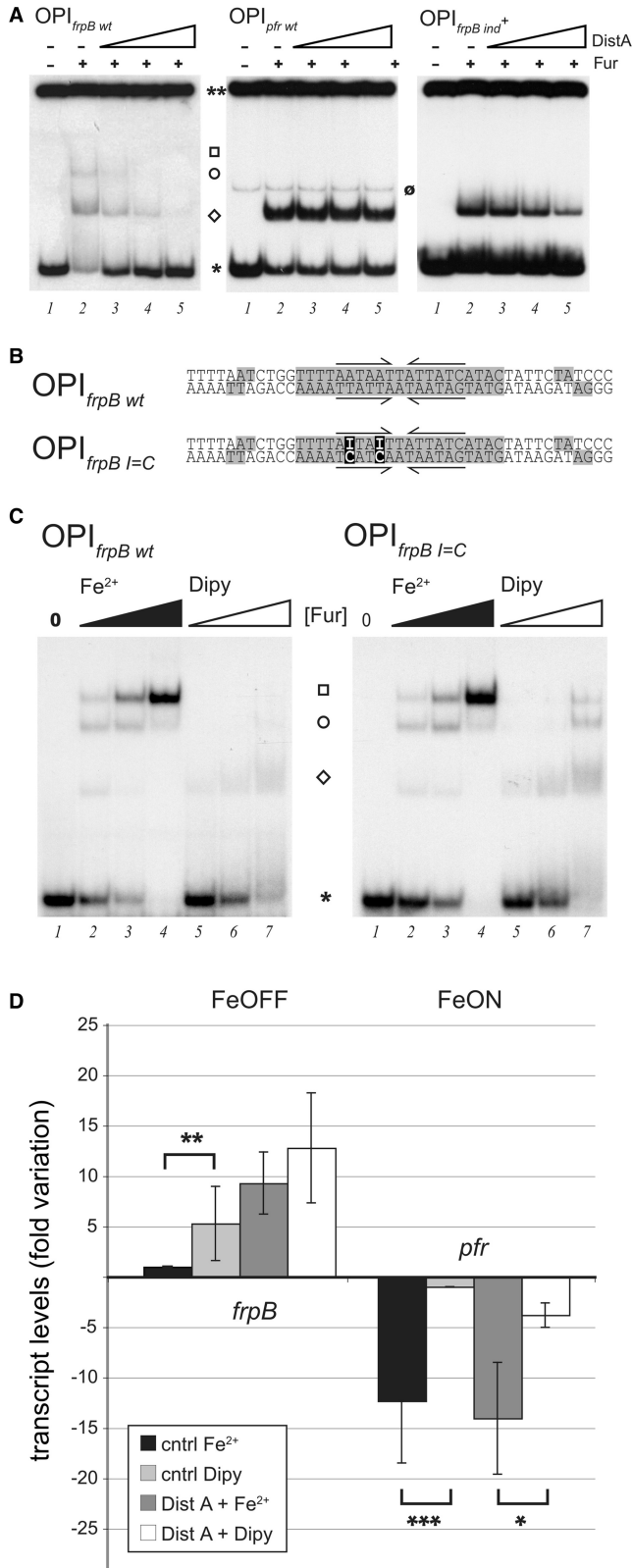
Figure 6. Minor groove readout in iron-repressible Fur regulation. (**A**) Distamycin A interference assays *in vitro* with OPI$_{frpB}$, OPI$_{pfr}$ and OPI$_{frpB\ ind}$+ operator probes. Lane 1, free probe. Lane 2, Fur-DNA complexes formed in the absence of distamycin A. Lanes 3–5, Fur-DNA complexes formed in the presence of 1.2, 2.4 and 4.8 nM distamycin A, respectively. Symbols are as in Figure 2. (**B**) I-C box substitutions of OPI$_{frpB}$ in OPI$_{frpB\ I=C}$ are shaded in black. Nucleotides

with the observation that Fur can tetramerize and further multimerize even in the absence of DNA. In the model, the resulting Fur tetramer does not interact with the DNA helix perpendicularly to the operator major axes, but is tilted by ∼30°, allowing both Fur dimers to interact with DNA regions that are weakly protected in •OH footprinting assay *in vitro* (Figure 4A, light grey triangles). In conclusion, these structural models are consistent with the experimental data and provide a molecular basis to understand how *Hp*Fur can bind two different operator motifs through different oligomeric states and discriminative readout of their DNA grooves.
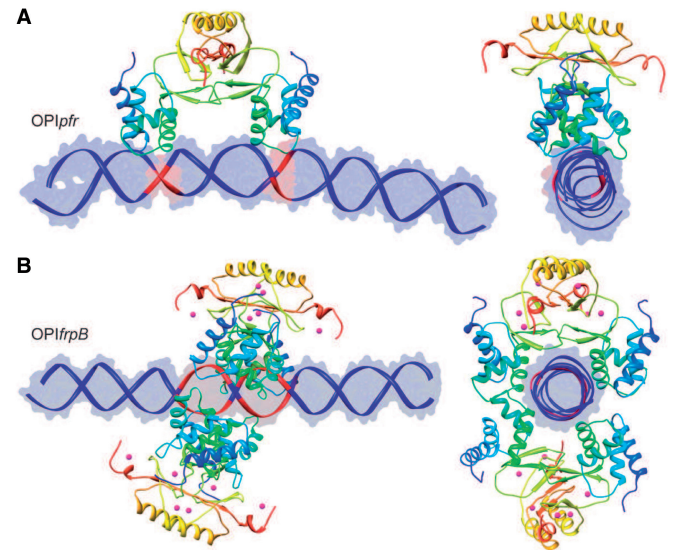
Figure 7. Fur-DNA interaction models. Best docking models resulting for Fur-OPI$_{pfr}$ (**A**) and Fur-OPI$_{frpB}$ (**B**) complexes (coloured in the online version). The protein is reported as ribbon diagram coloured from deep blue in the proximity of the N-terminal to red at the C-terminus. Zn^{2+} ions are reported as purple spheres. The DNA is reported as ribbon coloured in blue, with exception of the active residues, reported in red.

Figure 6. Continued
protected from •OH cleavage are shaded in grey. Arrows above the nucleotide sequences indicate the inverted repeat of the *holo*-operator consensus motif. (**C**) EMSA of OPI$_{frpB}$ (left panel) and I-C-substituted OPI$_{frpB\ I=C}$ probes with increasing concentrations of Fur in the presence of either 150 µM iron (Fe^{2+}) or 150 µM 2,2 dipyridyl (Dipy). Lane 1: free probe, 0 nM Fur (*); lanes 2–4 and 5–7, 19, 38 and 190 nM Fur dimer, respectively. Open diamond, circle and square indicate HMC, LMC and LMC2 Fur-DNA complexes, respectively. (**D**) Effects of distamycin A on iron-dependent Fur repression of *frpB* and *pfr*. Transcript levels were quantified by qRT-PCR on RNA extracted from mid-log *H. pylori* G27 cultures treated 15 min with 1 mM soluble Fe^{2+} or 150 µM 2,2 dipyridyl (Dipy), after 20 min preincubation with ddH$_2$O (cntrl) or 20 µM distamycin A (Dist A). The housekeeping gene *ppk* was used as control. To take in account only Fur-dependent responses, results were normalized to *frpB* and *pfr* transcript levels observed in the G27Δ*fur* strain under the same conditions. Statistically significant differences were assessed by Student's *t*-test. Error bars indicate the standard deviation deriving from two independent biological duplicates, each analysed twice in independent qRT-PCR runs, in triplicate technical replicates for each sample.

DISCUSSION

The struggle for iron as an essential element for cell growth and proliferation has a profound impact on the expression of virulence genes and on the control of central metabolic processes in many bacterial species and pathogens (6). As such, insights into the mechanisms of Fur-family regulators may contribute to the development of better therapeutic strategies and novel biotechnological applications targeting bacterial metal homeostasis.

Our results provide compelling evidence that in *H. pylori* Fur the mechanism of *holo*- or *apo*-regulation relies on different multimeric states and binding architectures of the regulator to its DNA elements. We show that allosteric changes induced by the Fe^{2+} cofactor enable the discriminative readout of either sequence and/or structural determinants that reside in *cis* on distinct *apo*- or *holo*-operators sequences. We demonstrate that specific Fur binding to the OPI$_{frpB}$ *holo*-operator requires multiple AAT triplet repeats. The lack of effect of I-C substitutions within these triplets on Fur binding can be interpreted either as a readout of minor groove determinants or as an indication that motif recognition is distributed over several binding sites, and that additional favorable protein–DNA and protein–protein interactions compensate for lost contacts in the major groove at the substitution sites. The results of distamycin interference, showing that minor groove binding of the drug outcompetes Fur binding to *holo*-operators, argue in favor of the first interpretation. Thus, considering the documented role of AAT trimers in narrowing the minor groove (38), as well as the different effect of distamycin A and I-C box substitutions on Fur regulation and operator binding, the AAT triplets of the *holo*-operator likely provide a discriminating feature for readout of critical minor groove determinants by the *holo*-Fur tetramer. On the contrary, Fur binding to the OPI$_{pfr}$ *apo*-operator appears to rely on interactions that occur primarily in the major groove, likely involving specific readout by *apo*-Fur of two thymine pairs spaced by one helical turn. According to this model, different orientations of the Fur DBDs relative to DNA may be involved in the discrimination of *apo*- and *holo*-operators. In this respect, it is interesting to recall that a peculiar orientation of the DBDs deduced from the *apo*-CjFur crystal structure has been suggested to underlie *apo*-regulation in *C. jejuni* Fur (17).

Compared with orthologs from other organisms, the Fur proteins of *H. pylori* and *C. jejuni* exhibit an N-terminal extension of 9–10 amino acids immediately up-stream of the DBD, forming an α-helix important for function (12,17,29,34). It is plausible that *apo*-Fur regulation depends on this specific N-terminal extension. In this regard, it is interesting that Fur regulated sRNAs, like PrrF or RyhB, have not been described in *H. pylori* and *C. jejuni* to date. This absence may be functionally compensated by *apo*-regulation and/or by the unique N-terminal extension of Fur proteins in these bacterial species.

In *Bacillus subtilis*, different mutlimerization states of Fur are involved in binding to naturally occurring operator sites, and it has been proposed that binding to opposed faces of the DNA element may account for these observations (43). Interestingly, *B. subtilis* Fur recognizes a TGATAAT half-site, and modifications to TTATAAT switch repression to the PerR paralog, while modifications to TCGTAAT switch to Zur repression. These results suggested that one half-site may be a discriminating contact point for Fur paralogs (44). Intriguingly, in *H. pylori* changes of TAATAAT into TAATGAT (the 'inside' half-site of the *holo*-operator) would form on the complementary strand a TCATT motif characteristic of the *apo*-operator. This may indicate interesting parallels between Fur paralog discrimination in *B. subtilis*, and *apo*- and *holo*-Fur repression in *H. pylori*. In addition, an •OH protection pattern covering the hexameric arrays of the GAT AAT sequence in a synthetic Fur-box has been reported for *holo*-Fur in *E. coli* (45). Thus, our observations shed light on the longstanding puzzle of *apo*- and *holo*-Fur regulation in the human pathogen *H. pylori* and provide significant advances to understand the mechanisms of Fur regulation in other prokaryotes.

In a broader context, our results explain how multiple DNA elements can be recognized by a single transcription factor in different conformations and with alternate regulatory outcomes. For example, recent structural and biochemical studies on *E. coli* IscR have shown that binding of the Fe-S cofactor to the protein broadens its DNA binding specificity from *apo*-operator motifs only to both *apo*- and *holo*-operator sequences, expanding the DNA target selection, and thereby the regulatory potential of the transcription factor (20). In analogy to IscR, we propose that *Hp*Fur multimerization induced by Fe^{2+} cofactor binding promotes a remodelling of the protein–DNA interface, which allows for the discriminative recognition AT-rich *holo*-operator motifs over *apo*-operators. The mutagensis of key residues at the dimer–dimer Fur interaction surface impairs the affinity towards *holo*-operators significantly more than towards *apo*-operators (D. Roncarati and A. Danielli; unpublished data), supporting the proposed structural model of Fur-DNA interactions, in which a *holo*-Fur tetramer is predicted to clamp the DNA helix.

Finally, the mechanism we describe appears to involve the discriminative readout of determinants carried on the two grooves of the DNA. It accounts for the ability of *Hp*Fur to function as a Fe^{2+}-responsive molecular commutator switch, to concomitantly regulate alternative sets of Fe^{2+}-inducible and Fe^{2+}-repressible promoters in *H. pylori*. Given the poor GC-content of its genome, this mechanism may have evolved to compensate for the paucity of regulators and control transcription of AT-rich loci, exploiting Fur to readout also the minor groove features imposed by recurrent AT-tracts. The importance of minor groove readout is becoming evident in an increasing number of transcription factors. Base- or shape-specific contacts in the minor groove of AT-rich sequences have been demonstrated for several DNA binding proteins. In AT-hooks, extended arm sequences and homeodomains these interactions involve short peptide motifs containing arginine residues that contact bases in the minor groove (46). Some of these proteins, such as the TATA-box

binding protein TBP (47) or the integration host factor IHF (48), readout the DNA sequence exclusively through the minor groove. Other proteins are able to interact with both the minor and the major groove of the DNA e.g. MogR repressor of *Listeria monocytogenes* (49), Hin recombinase (50) and THAP proteins (51). *Hp*Fur, therefore, adds to this list of regulators able to readout specific determinants also in the minor groove. This has interesting implications, as minor groove binding drugs have been suggested as alternative treatment approaches for critical pathologies and successfully used for targeting the minor groove-binding transcription factors involved in disease (39,52).

Most importantly, *H. pylori* Fur represents, to the best of our knowledge, the first example of a regulator that is able to recognize distinct motifs by discriminative readout of genetic determinants carried on the two DNA grooves to transduce the same regulatory input (Fe^{2+}) in opposite transcriptional outputs (FeON-FeOFF). As such, it represents a novel regulatory paradigm that further expands our fundamental knowledge on gene regulation and transcriptional commutator switches.

SUPPLEMENTARY DATA

Supplementary Data are available at NAR Online, including [53–68].

ACKNOWLEDGEMENTS

FUNDING

REFERENCES

1. Jacob,F. and Monod,J. (1961) Genetic regulatory mechanisms in the synthesis of proteins. *J. Mol. Biol.*, **3**, 318–356.
2. Müller,J., Oehler,S. and Müller-Hill,B. (1996) Repression of lac promoter as a function of distance, phase and quality of an auxiliary lac operator. *J. Mol. Biol.*, **257**, 21–29.
3. Youderian,P. and Arvidson,D.N. (1994) Direct recognition of the trp operator by the trp holorepressor—a review. *Gene*, **150**, 1–8.
4. Baron,U., Schnappinger,D., Helbl,V., Gossen,M., Hillen,W. and Bujard,H. (1999) Generation of conditional mutants in higher eukaryotes by switching between the expression of two genes. *Proc. Natl Acad. Sci. USA*, **96**, 1013–1018.
5. O'Halloran,T.V. (1993) Transition metals in control of gene expression. *Science*, **261**, 715–725.
6. Nairz,M., Schroll,A., Sonnweber,T. and Weiss,G. (2010) The struggle for iron—a metal at the host-pathogen interface. *Cell. Microbiol.*, **12**, 1691–1702.
7. Carpenter,B.M., Whitmire,J.M. and Merrell,D.S. (2009) This is not your mother's repressor: the complex role of fur in pathogenesis. *Infect. Immun.*, **77**, 2590–2601.
8. Danielli,A. and Scarlato,V. (2010) Regulatory circuits in *Helicobacter pylori*: network motifs and regulators involved in metal-dependent responses. *FEMS Microbiol. Rev.*, **34**, 738–752.
9. Bagg,A. and Neilands,J.B. (1987) Ferric uptake regulation protein acts as a repressor, employing iron (II) as a cofactor to bind the operator of an iron transport operon in *Escherichia coli*. *Biochemistry*, **26**, 5471–5477.
10. Delany,I., Spohn,G., Rappuoli,R. and Scarlato,V. (2001) The Fur repressor controls transcription of iron-activated and -repressed genes in *Helicobacter pylori*. *Mol. Microbiol.*, **42**, 1297–1309.
11. Bereswill,S., Greiner,S., Van Vliet,A.H., Waidner,B., Fassbinder,F., Schiltz,E., Kusters,J.G. and Kist,M. (2000) Regulation of ferritin-mediated cytoplasmic iron storage by the ferric uptake regulator homolog (Fur) of *Helicobacter pylori*. *J. Bacteriol.*, **182**, 5948–5953.
12. Gilbreath,J.J., Pich,O.Q., Benoit,S.L., Besold,A.N., Cha,J.H., Maier,R.J., Michel,S.L.J., Maynard,E.L. and Merrell,D.S. (2013) Random and site-specific mutagenesis of the *Helicobacter pylori* ferric uptake regulator provides insight into Fur structure-function relationships. *Mol. Microbiol.*, **89**, 304–323, 10.1111/mmi.12278.
13. Carpenter,B.M., Gancz,H., Gonzalez-Nieves,R.P., West,A.L., Whitmire,J.M., Michel,S.L.J. and Merrell,D.S. (2009) A single nucleotide change affects fur-dependent regulation of sodB in *H pylori*. *PLoS One*, **4**, e5369.
14. Ernst,F.D., Homuth,G., Stoof,J., Mäder,U., Waidner,B., Kuipers,E.J., Kist,M., Kusters,J.G., Bereswill,S. and Van Vliet,A.H.M. (2005) Iron-responsive regulation of the *Helicobacter pylori* iron-cofactored superoxide dismutase SodB is mediated by Fur. *J. Bacteriol.*, **187**, 3687–3692.
15. Delany,I., Spohn,G., Pacheco,A.B.F., Ieva,R., Alaimo,C., Rappuoli,R. and Scarlato,V. (2002) Autoregulation of *Helicobacter pylori* Fur revealed by functional analysis of the iron-binding site. *Mol. Microbiol.*, **46**, 1107–1122.
16. Delany,I., Spohn,G., Rappuoli,R. and Scarlato,V. (2003) An anti-repression Fur operator upstream of the promoter is required for iron-mediated transcriptional autoregulation in *Helicobacter pylori*. *Mol. Microbiol.*, **50**, 1329–1338.
17. Butcher,J., Sarvan,S., Brunzelle,J.S., Couture,J.-F. and Stintzi,A. (2012) Structure and regulon of Campylobacter jejuni ferric uptake regulator Fur define apo-Fur regulation. *Proc. Natl Acad. Sci. USA*, **109**, 10047–10052.
18. Teramoto,H., Inui,M. and Yukawa,H. (2012) Corynebacterium glutamicum Zur acts as a zinc-sensing transcriptional repressor of both zinc-inducible and zinc-repressible genes involved in zinc homeostasis. *FEBS J.*, **279**, 4385–4397.
19. Nesbit,A.D., Giel,J.L., Rose,J.C. and Kiley,P.J. (2009) Sequence-specific binding to a subset of IscR-regulated promoters does not require IscR Fe-S cluster ligation. *J. Mol. Biol.*, **387**, 28–41.
20. Rajagopalan,S., Teter,S.J., Zwart,P.H., Brennan,R.G., Phillips,K.J. and Kiley,P.J. (2013) Studies of IscR reveal a unique mechanism for metal-dependent regulation of DNA binding specificity. *Nat. Struct. Mol. Biol.*, **20**, 740–747.
21. Danielli,A., Amore,G. and Scarlato,V. (2010) Built shallow to maintain homeostasis and persistent infection: insight into the transcriptional regulatory network of the gastric human pathogen *Helicobacter pylori*. *PLoS Pathog.*, **6**, e1000938.

22. Danielli,A., Roncarati,D., Delany,I., Chiarini,V., Rappuoli,R. and Scarlato,V. (2006) *In vivo* dissection of the *Helicobacter pylori* Fur regulatory circuit by genome-wide location analysis. *J. Bacteriol.*, **188**, 4654–4662.

23. Gancz,H., Censini,S. and Merrell,D.S. (2006) Iron and pH homeostasis intersect at the level of Fur regulation in the gastric pathogen *Helicobacter pylori*. *Infect. Immun.*, **74**, 602–614.

24. Pich,O.Q., Carpenter,B.M., Gilbreath,J.J. and Merrell,D.S. (2012) Detailed analysis of *Helicobacter pylori* Fur-regulated promoters reveals a Fur box core sequence and novel Fur-regulated genes. *Mol. Microbiol.*, **84**, 921–941.

25. Friedman,Y.E. and O'Brian,M.R. (2003) A novel DNA-binding site for the ferric uptake regulator (Fur) protein from Bradyrhizobium japonicum. *J. Biol. Chem.*, **278**, 38395–38401.

26. Ouyang,Z., Deka,R.K. and Norgard,M.V. (2011) BosR (BB0647) controls the RpoN-RpoS regulatory pathway and virulence expression in Borrelia burgdorferi by a novel DNA-binding mechanism. *PLoS Pathog.*, **7**, e1001272.

27. Danielli,A., Romagnoli,S., Roncarati,D., Costantino,L., Delany,I. and Scarlato,V. (2009) Growth phase and metal-dependent transcriptional regulation of the fecA genes in *Helicobacter pylori*. *J. Bacteriol.*, **191**, 3717–3725.

28. Roncarati,D., Danielli,A., Spohn,G., Delany,I. and Scarlato,V. (2007) Transcriptional regulation of stress response and motility functions in helicobacter pylop.12 ri is mediated by HspR and HrcA. *J. Bacteriol.*, **189**, 7234–7243.

29. Dian,C., Vitale,S., Leonard,G.A., Bahlawane,C., Fauquant,C., Leduc,D., Muller,C., De Reuse,H., Michaud-Soret,I. and Terradot,L. (2011) The structure of the *Helicobacter pylori* ferric uptake regulator Fur reveals three functional metal binding sites. *Mol. Microbiol.*, **79**, 1260–1275.

30. Wiederstein,M. and Sippl,M.J. (2007) ProSA-web: interactive web service for the recognition of errors in three-dimensional structures of proteins. *Nucleic Acids Res.*, **35**, W407–W410.

31. Suhre,K. and Sanejouand,Y.-H. (2004) ElNemo: a normal mode web server for protein movement analysis and the generation of templates for molecular replacement. *Nucleic Acids Res.*, **32**, W610–W614.

32. Van Dijk,M. and Bonvin,A.M.J.J. (2009) 3D-DART: a DNA structure modelling server. *Nucleic Acids Res.*, **37**, W235–W239.

33. Van Dijk,M., Van Dijk,A.D.J., Hsu,V., Boelens,R. and Bonvin,A.M.J.J. (2006) Information-driven protein-DNA docking using HADDOCK: it is a matter of flexibility. *Nucleic Acids Res.*, **34**, 3317–3325.

34. Carpenter,B.M., Gancz,H., Benoit,S.L., Evans,S., Olsen,C.H., Michel,S.L.J., Maier,R.J. and Merrell,D.S. (2010) Mutagenesis of conserved amino acids of *Helicobacter pylori* fur reveals residues important for function. *J. Bacteriol.*, **192**, 5037–5052.

35. Thomas-Chollier,M., Defrance,M., Medina-Rivera,A., Sand,O., Herrmann,C., Thieffry,D. and Van Helden,J. (2011) RSAT 2011: regulatory sequence analysis tools. *Nucleic Acids Res.*, **39**, W86–W91.

36. Delany,I., Ieva,R., Soragni,A., Hilleringmann,M., Rappuoli,R. and Scarlato,V. (2005) *In vitro* analysis of protein-operator interactions of the NikR and fur metal-responsive regulators of coregulated genes in *Helicobacter pylori*. *J. Bacteriol.*, **187**, 7703–7715.

37. Bishop,E.P., Rohs,R., Parker,S.C.J., West,S.M., Liu,P., Mann,R.S., Honig,B. and Tullius,T.D. (2011) A map of minor groove shape and electrostatic potential from hydroxyl radical cleavage patterns of DNA. *ACS Chem. Biol.*, **6**, 1314–1320.

38. Rohs,R., West,S.M., Sosinsky,A., Liu,P., Mann,R.S. and Honig,B. (2009) The role of DNA shape in protein-DNA recognition. *Nature*, **461**, 1248–1253.

39. Raskatov,J.A., Meier,J.L., Puckett,J.W., Yang,F., Ramakrishnan,P. and Dervan,P.B. (2012) Modulation of NF-κB-dependent gene transcription using programmable DNA minor groove binders. *Proc. Natl Acad. Sci. USA*, **109**, 1023–1028.

40. Lankas,F., Cheatham,T.E. 3rd, Spacková,N., Hobza,P., Langowski,J. and Sponer,J. (2002) Critical effect of the N2 amino group on structure, dynamics, and elasticity of DNA polypurine tracts. *Biophys. J.*, **82**, 2592–2609.

41. Dominguez,C., Boelens,R. and Bonvin,A.M.J.J. (2003) HADDOCK: a protein-protein docking approach based on biochemical or biophysical information. *J. Am. Chem. Soc.*, **125**, 1731–1737.

42. De Vries,S.J., Van Dijk,A.D.J., Krzeminski,M., Van Dijk,M., Thureau,A., Hsu,V., Wassenaar,T. and Bonvin,A.M.J.J. (2007) HADDOCK versus HADDOCK: new features and performance of HADDOCK2.0 on the CAPRI targets. *Proteins*, **69**, 726–733.

43. Baichoo,N. and Helmann,J.D. (2002) Recognition of DNA by Fur: a reinterpretation of the Fur box consensus sequence. *J. Bacteriol.*, **184**, 5826–5832.

44. Fuangthong,M. and Helmann,J.D. (2003) Recognition of DNA by three ferric uptake regulator (Fur) homologs in Bacillus subtilis. *J. Bacteriol.*, **185**, 6348–6357.

45. Escolar,L., Pérez-Martín,J. and De Lorenzo,V. (1998) Binding of the fur (ferric uptake regulator) repressor of *Escherichia coli* to arrays of the GATAAT sequence. *J. Mol. Biol.*, **283**, 537–547.

46. Rohs,R., Jin,X., West,S.M., Joshi,R., Honig,B. and Mann,R.S. (2010) Origins of specificity in protein-DNA recognition. *Annu. Rev. Biochem.*, **79**, 233–269.

47. Kim,J.L., Nikolov,D.B. and Burley,S.K. (1993) Co-crystal structure of TBP recognizing the minor groove of a TATA element. *Nature*, **365**, 520–527.

48. Rice,P.A., Yang,S., Mizuuchi,K. and Nash,H.A. (1996) Crystal structure of an IHF-DNA complex: a protein-induced DNA U-turn. *Cell*, **87**, 1295–1306.

49. Shen,A., Higgins,D.E. and Panne,D. (2009) Recognition of AT-rich DNA binding sites by the MogR repressor. *Structure*, **17**, 769–777.

50. Feng,J.A., Johnson,R.C. and Dickerson,R.E. (1994) Hin recombinase bound to DNA: the origin of specificity in major and minor groove interactions. *Science*, **263**, 348–355.

51. Sabogal,A., Lyubimov,A.Y., Corn,J.E., Berger,J.M. and Rio,D.C. (2010) THAP proteins target specific DNA sites through bipartite recognition of adjacent major and minor grooves. *Nat. Struct. Mol. Biol.*, **17**, 117–123.

52. Baron,R.M., Lopez-Guzman,S., Riascos,D.F., Macias,A.A., Layne,M.D., Cheng,G., Harris,C., Chung,S.W., Reeves,R., Von Andrian,U.H. *et al.* (2010) Distamycin A inhibits HMGA1-binding to the P-selectin promoter and attenuates lung and liver inflammation during murine endotoxemia. *PLoS One*, **5**, e10656.

53. Vitale,S., Fauquant,C., Lascoux,D., Schauer,K., Saint-Pierre,C. and Michaud-Soret,I. (2009) A ZnS(4) structural zinc site in the *Helicobacter pylori* ferric uptake regulator. *Biochemistry*, **48**, 5582–5591.

54. Zambelli,B., Musiani,F. and Ciurli,S. (2012) Metal ion-mediated DNA-protein interactions. *Met Ions Life Sci*, **10**, 135–170.

55. Roncarati,D., Danielli,A. and Scarlato,V. (2011) CbpA acts as a modulator of HspR repressor DNA binding activity in *Helicobacter pylori*. *J. Bacteriol.*, **193**, 5629–5636.

56. Crooks,G.E., Hon,G., Chandonia,J.-M. and Brenner,S.E. (2004) WebLogo: a sequence logo generator. *Genome Res.*, **14**, 1188–1190.

57. Orchard,K. and May,G.E. (1993) An EMSA-based method for determining the molecular weight of a protein-DNA complex. *Nucleic Acids Res.*, **21**, 3335–3336.

58. Cui,Y., Midkiff,M.A., Wang,Q. and Calvo,J.M. (1996) The leucine-responsive regulatory protein (Lrp) from *Escherichia coli*. Stoichiometry and minimal requirements for binding to DNA. *J. Biol. Chem.*, **271**, 6611–6617.

59. Tullius,T.D. and Dombroski,B.A. (1986) Hydroxyl radical 'footprinting': high-resolution information about DNA-protein contacts and application to lambda repressor and Cro protein. *Proc. Natl Acad. Sci. USA.*, **83**, 5469–5473.

60. Liu,S.T. and Hong,G.F. (1998) Three-minute G+A specific reaction for DNA sequencing. *Anal. Biochem.*, **255**, 158–159.

61. Churchill,M.E., Hayes,J.J. and Tullius,T.D. (1990) Detection of drug binding to DNA by hydroxyl radical footprinting. Relationship of distamycin binding sites to DNA structure and positioned nucleosomes on 5S RNA genes of Xenopus. *Biochemistry*, **29**, 6043–6050.

62. Muller,C., Bahlawane,C., Aubert,S., Delay,C.M., Schauer,K., Michaud-Soret,I. and De Reuse,H. (2011) Hierarchical regulation of the NikR-mediated nickel response in *Helicobacter pylori*. *Nucleic Acids Res.*, **39**, 7564–7575.

63. Sali,A. and Blundell,T.L. (1993) Comparative protein modelling by satisfaction of spatial restraints. *J. Mol. Biol.*, **234**, 779–815.

64. Shen,M.-Y. and Sali,A. (2006) Statistical potential for assessment and prediction of protein structures. *Protein Sci.*, **15**, 2507–2524.

65. Pohl,E., Haller,J.C., Mijovilovich,A., Meyer-Klaucke,W., Garman,E. and Vasil,M.L. (2003) Architecture of a protein central to iron homeostasis: crystal structure and spectroscopic analysis of the ferric uptake regulator. *Mol. Microbiol.*, **47**, 903–915.

66. Sheikh,M.A. and Taylor,G.L. (2009) Crystal structure of the Vibrio cholerae ferric uptake regulator (Fur) reveals insights into metal co-ordination. *Mol. Microbiol.*, **72**, 1208–1220.

67. Tiss,A., Barre,O., Michaud-Soret,I. and Forest,E. (2005) Characterization of the DNA-binding site in the ferric uptake regulator protein from *Escherichia coli* by UV crosslinking and mass spectrometry. *FEBS Lett.*, **579**, 5454–5460.

68. Toledo,H., Villafaena,C., Valenzuela,M. and López-Solís,R. (2012) Arginine 66 residue of Fur is required for the regulatory function of this protein in the acid adaptation mechanism of *Helicobacter pylori*. *Helicobacter*, **17**, 16–22.